Research Reports: Biological

Niche Specific Microbiota-Dependent and Independent Bone Loss around Dental Implants and Teeth

O. Heyman[1], Y. Horev[1], N. Koren[2], O. Barel[2], I. Aizenbud[2],
Y. Aizenbud[2], M. Brandwein[2], L. Shapira[1], A.H. Hovav[2],
and A. Wilensky[1]

Abstract

Oral mucosal homeostasis is achieved by complex immunologic mechanisms, orchestrating host immunity to adapt to the physiologic functions of the various specialized niches in the oral cavity. Dental implants introduce a novel mucosal niche to the immune system to deal with. Nevertheless, the immune mechanisms engaged toward implants and whether they have broader effects are not well defined. Using a murine model, we found an accumulation of neutrophils and RANKL-expressing T and B lymphocytes in the implant-surrounding mucosa, accompanied by local bone loss. Surprisingly, the presence of implants had an impact on remote periodontal sites, as elevated inflammation and accelerated bone loss were detected in intact distant teeth. This was due to microbial dysbiosis induced by the implants, since antibiotic treatment prevented bone loss around teeth. However, antibiotic treatment failed to prevent the loss of implant-supporting bone, highlighting the distinct mechanisms mediating bone loss at each site. Further analysis revealed that implants induced chronic lymphocyte activation and increased mRNA expression of IFN-α and accumulation of IFN-α–producing plasmacytoid dendritic cells, which we previously reported as bone-destructive immune responses. Collectively, this study demonstrates that implants have a strong and broad impact on oral mucosal homeostasis, inducing periodontal bone loss in a niche-specific manner that is both microbiota dependent and independent.

Keywords: peri-implantitis, peri-implant mucosa, marginal bone loss, immune homeostasis, bacterial dysbiosis, plasmacytoid dendritic cells

Introduction

The oral cavity is a complex ecosystem involving constant host-bacteria interactions that shape local immune responses to maintain mucosal homeostasis (Hajishengallis et al. 2011). This delicate balance is often dysregulated, resulting in uncontrolled immune responses that could lead to oral and systemic pathologies (Hovav 2014; Hajishengallis et al. 2016). Periodontitis represents one of the most common inflammatory diseases that culminate in the destruction of the periodontal apparatus (Armitage 1996). It has been established that bacterial plaque is the main etiologic factor mediating excessive immune responses and, consequently, periodontal bone destruction (Van Dyke et al. 1993). Furthermore, a recent study reported that under physiologic conditions, ongoing damage to the oral epithelium due to masticatory forces facilitates local expansion of Th17 cells and induces alveolar bone destruction in a microbiota-independent manner (Dutzan et al. 2017). The importance of the oral epithelium in regulating mucosal homeostasis and bone loss was also demonstrated in mice lacking the protein growth arrest–specific 6 (GAS6; Nassar et al. 2017). Expression of GAS6 is upregulated in the oral epithelium postnatally by the microbiota, where it acts as a central regulator of host-bacteria interplay. These observations suggest that alveolar bone loss around teeth can be mediated by various mechanisms under physiologic or inflammatory conditions.

Peri-implantitis is an additional oral inflammatory disease involving bone destruction around dental implants (Berglundh et al. 2011; Berglundh et al. 2018) and is considered a major global health concern (Derks and Tomasi 2015). Although the primary etiology of this disease associates with the microbiota, we have shown that titanium implants by themselves can elevate the local inflammatory milieu and dysregulate mucosal homeostasis. This effect is mediated by titanium ions released

[1]Department of Periodontology, Faculty of Dental Medicine, Hebrew University–Hadassah Medical Center, Jerusalem, Israel
[2]The Institute of Dental Sciences, Faculty of Dental Medicine, Hebrew University, Jerusalem, Israel

A supplemental appendix to this article is available online.

Corresponding Author:
A. Wilensky, Department of Periodontology, Faculty of Dental Medicine, Hebrew University-Hadassah Medical Center, PO Box 12272, Jerusalem 91120, Israel.
Email: asafw@ekmd.huji.ac.il

from the implants, which impair the development of Langerhans cells that function as regulators of oral mucosal immunity (Heyman et al. 2018). Nevertheless, despite the assumption that peri-implantitis and periodontitis share etiologic factors and hence are treated similarly, periodontitis generally responds well to bacterial plaque control while peri-implantitis is much less responsive (Renvert et al. 2008). Moreover, whereas antibiotic treatment is beneficial in the treatment of periodontitis, its efficacy in peri-implantitis is debatable (Javed et al. 2013; Romanos et al. 2015). This suggests that although the clinical signs of both diseases are similar, the immune mechanisms and the role of microbiota in each disease are likely to be different.

Using a murine model of dental implants, we found in the current study that besides increasing local inflammation and bone loss, implants are capable to induce oral microbial dysbiosis and enhance inflammation and bone loss in remote teeth. This enabled us to dissect the mechanisms mediating bone loss around implants and teeth under physiologic conditions. Our data suggest that bone loss in each niche involves distinct immunologic and microbial mechanisms, highlighting the specificity and complexity of the oral immune system.

Materials and Methods

Mice

Female BALB/c mice (4 to 5 wk old) were purchased from Envigo. The animals were housed in the specific pathogen–free unit. All experimental procedures were reviewed and approved by the Institutional Animal Care and Use Committee of the Hebrew University-Hadassah Medical Center and followed the ARRIVE guidelines.

Extractions and Implant Placement

The model design and surgery protocols used for this study were previously described (Heyman et al. 2018). For details, see Appendix.

Isolation and Processing the Gingiva and Peri-implant Mucosal Tissues

The mucosal tissues were processed as previously reported (Heyman et al. 2018) and are described in the Appendix.

RNA Extraction and Quantitative Real-time Polymerase Chain Reaction

RNA was isolated and processed via quantitative real-time polymerase chain reaction (RT-qPCR; see Appendix).

Antibodies and Reagents

Antibodies and reagents are described in the Appendix.

Micro–computed tomography Analysis

For micro–computed tomography scans and bone analysis for teeth and implants, see Appendix.

Cytokine Secretion by Cultured Splenocytes

The supernatants of cultured splenocytes were analyzed by ELISA (see Appendix).

Cultivation of Oral Microbiota

The oral cavity of each mouse was swabbed for 30 s, and the samples were plated as outlined in the Appendix.

Microbiome Sequencing and Analysis

Oral bacterial DNA was extracted and used for Illumina sequencing, as described in the Appendix, with data analysis and diversity-related statistical tests.

Broad-Spectrum Antibiotic Model

Four antibiotics and an antifungal treatment were administrated to the mice. For details, see Appendix.

Statistical Analysis

In each experiment, the mice were independently tested and data expressed as mean ± SEM. Statistical tests were performed with the Student t test. $P < 0.05$ was considered significant.

Results

Dental Implants Promote Bone Loss around Remote Teeth

We have previously shown that titanium dental implants impair local development of Langerhans cells, resulting in elevated inflammation at the implant vicinity (Heyman et al. 2018). To examine if the presence of such dysregulated local immunity affects the implant-supporting bone, we evaluated bone volume at various time points after implant placement using micro–computed tomography (Fig. 1A). As demonstrated in Figure 1B and C, we detected gradual bone loss at 4 and 10 wk after implant placement as compared with 2-wk controls. We then asked whether the implants were promoting alveolar bone loss around remote teeth. For this, we assessed the bone around the contralateral teeth 10 wk after implant placement; as a control, the same area in naïve mice was examined (Fig. 1D, E). Indeed, micro–computed tomography analysis revealed a significant reduction in bone volume around the contralateral teeth of implanted mice as compared with the teeth of nonimplanted mice. Since receptor activator of NF-κB ligand (RANKL) and its antagonist osteoprotegerin (OPG) are key
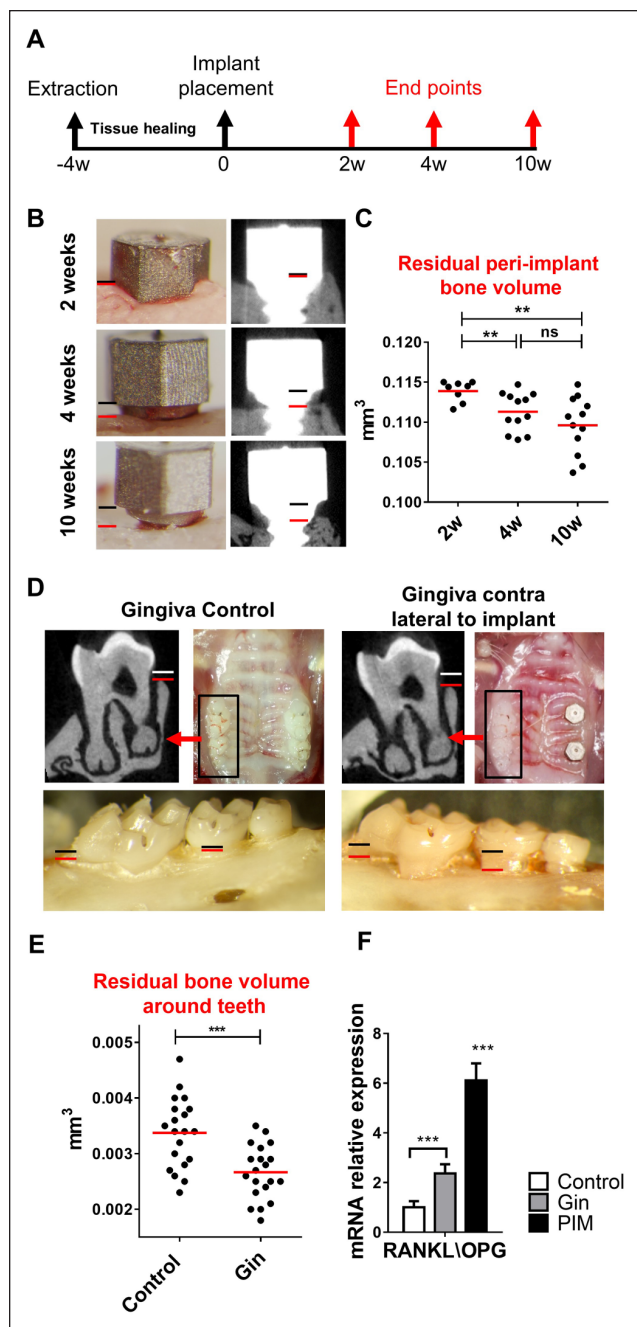
Figure 1. Bone resorption around implants and contralateral teeth following implant placement. (**A**) Experimental design. (**B**) Representative clinical and micro–computed tomography images at 2, 4, and 10 wk after implant placement. Bone loss is visible around the implant's neck. The black line represents the bone level at baseline, and the red line represents the bone level at each time point. (**C**) Three-dimensional quantification of the residual peri-implant bone volume over time. Dot plot graph illustrates 2 independent experiments with 32 mice (*n* = 8 to 12 mice per time point). Each dot represents the average residual bone volume of the 2 implants in 1 mouse. Red lines indicate the mean values for each time point. (**D**) Representative clinical and micro–computed tomography images of the contralateral teeth to the implants taken 10 wk after implant insertion. Bone loss is visible around the contralateral teeth. The black line marks the cementoenamel junction, and the red line represents the alveolar crest. (**E**) Three-dimensional quantification analysis of the residual bone volume around

regulators of pathophysiologic bone remodeling (Grimaud et al. 2003), we calculated the ratio of RANKL and OPG mRNA levels using RT-qPCR in the tissue. In concurrence with the bone loss results, the highest RANKL:OPG ratio was found around implants (peri-implant mucosa), whereas in the contralateral teeth (gingiva), the ratio was lower but still significantly higher than the teeth of naïve mice (control; Fig. 1F). Collectively, these findings suggest that dental implants undergo spontaneous bone loss with time. Moreover, the presence of the implant accelerates alveolar bone loss around remote teeth.

Implants Dysregulate Immune Homeostasis around Remote Teeth

We next characterized gingival leukocyte subpopulations that are known to regulate periodontal bone remodeling (Mizraji et al. 2017). The gating strategy is provided in Appendix Figure 1A. Four weeks after implant placement, total leukocytes (CD45$^+$) were significantly elevated around implants (peri-implant mucosa) and, to a lesser extent, in the contralateral teeth (gingiva) in comparison with gingiva of naïve mice (control; Fig. 2A). The same pattern was observed in the lymphoid lineage, with higher frequencies of T cells (CD3$^+$), B cells (B220$^+$), T-helper cells (CD3$^+$CD4$^+$), and T-regulatory cells (CD3$^+$CD4$^+$FoxP3$^+$) in the implant and contralateral teeth as compared with naïve control (Fig. 2B, C). Since expression of RANKL on lymphocytes was reported to affect osteoclastogenesis and facilitate bone loss (Chen et al. 2014), we evaluated its expression on T and B cells. Concurring with our earlier results regarding RANKL/OPG mRNA expression (Fig. 1F), RANKL expression on gingival CD4$^+$ T cells was elevated in implant and contralateral teeth; nevertheless, RANKL-expressing B cells increased only around implants (Fig. 2C). With regard to myeloid cells, neutrophils and Ly6C^{hi} and Ly6C^{lo} monocytes present at higher frequencies only around implants (Fig. 2D). To further examine the immunologic state of the mentioned tissues, we quantified by RT-qPCR the expression of certain immunologic genes 4 wk after implant placement. As depicted in Figure 2E, the expression of IFN-γ, IFN-α, and IL-1β was significantly upregulated in the peri-implant mucosa and contralateral teeth as compared with naïve mice. IL-17A and IFN-β expression, however, was elevated only in the peri-implant mucosa. Of note, no differences were found in the expression of genes involved in the recruitment of

teeth 10 wk after implant insertion. Each dot represents the residual bone volume of 1 mouse. Red lines indicate the mean values for each time point. Data are representative of 3 independent experiments of 40 mice (*n* = 20 per group). (**F**) Quantification of RANKL and osteoprotegerin mRNA ratio levels in the peri-implant mucosa (PIM), contralateral teeth (gingiva [GIN]), and gingiva in nonimplanted mice (control) per quantitative real-time polymerase chain reaction. Graph presents the fold change in gene expression normalized to control gingiva (nonimplanted mice) and presented as the mean ± SEM (*n* = 8 to 12 per group, each *n* represents oral tissues pooled from 2 individual mice). Data are representative of 2 independent experiments. **P < 0.01. ***P < 0.001.
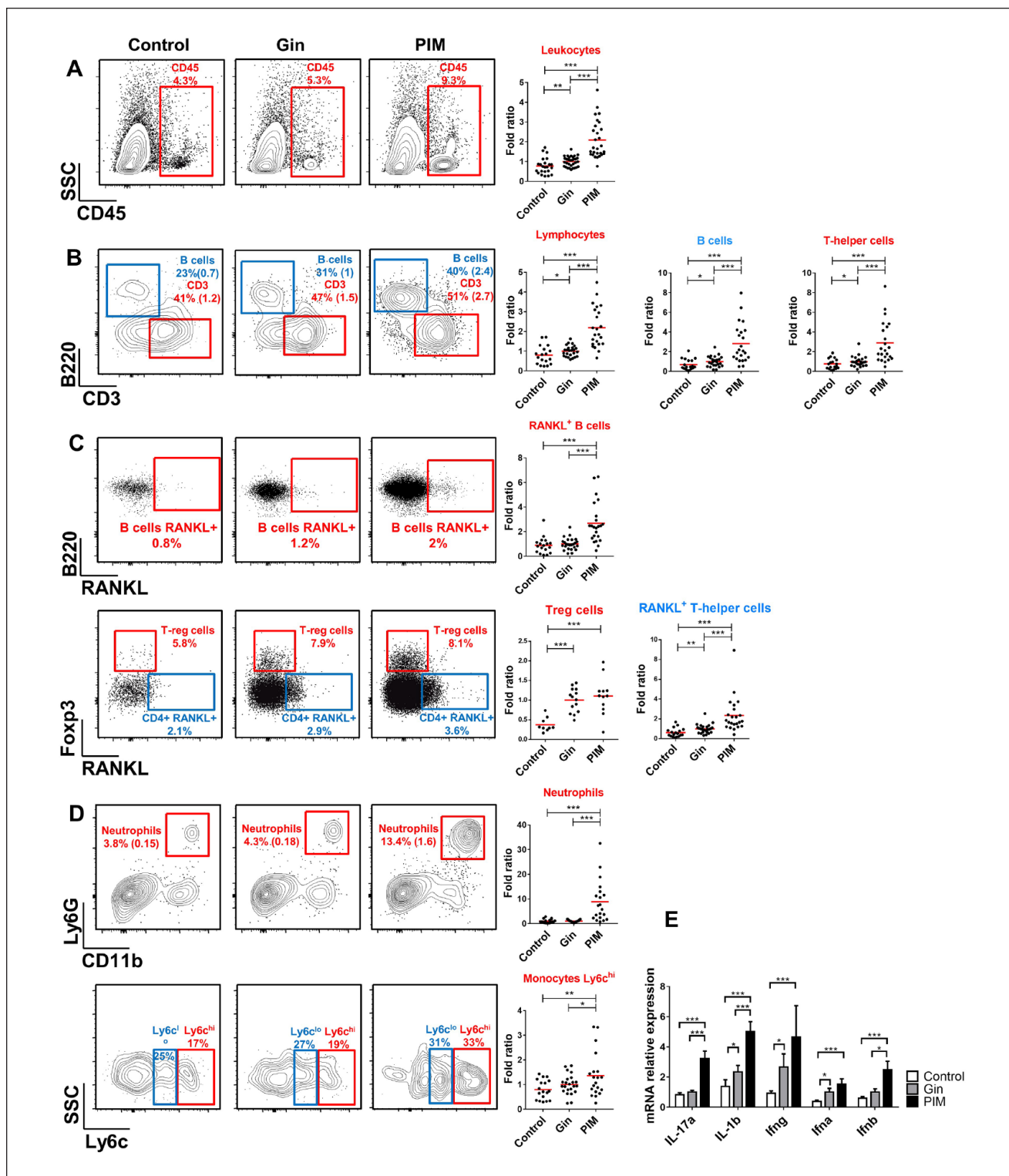
Figure 2. Implant placement dysregulated immune homeostasis in the tissue surrounding the implant and the contralateral teeth. Different immune cell populations were quantified in the gingiva of nonimplanted mice (control), contralateral gingiva of implanted mice (Gin), and peri-implant mucosa (PIM) per flow cytometry (FACS). Representative FACS plots show the frequencies of (**A**) CD45$^+$ leukocytes; (**B**) B cells (B220$^+$), total lymphocytes (CD3$^+$), T helper cells (CD3$^+$CD4$^+$); (**C**) RANKL expressing T cells (CD3$^+$CD4$^+$RANKL$^+$), B cells (B220$^+$RANKL$^+$), and Treg cells (CD3$^+$CD4$^+$FOXP3$^+$); and (**D**) neutrophils (Ly6G$^+$CD11b$^+$) and monocytes (CD11b$^+$Ly6C$^{high\backslash low}$). Dot graphs indicate the fold change in the percentage of each immune subtype from the total cell count, normalized to the Gin group (n = 9 to 32 per group; each n represents oral tissues pooled from 2 mice). Red lines indicate the mean values for each group. Data are representative of ≥3 independent experiments. (**E**) mRNA levels of the noted genes were quantified in the gingiva of nonimplanted mice (control), contralateral gingiva of implanted mice (Gin), and peri-implant mucosa (PIM) per quantitative real-time polymerase chain reaction. Graph presents the fold change in gene expression normalized to the Gin group and represents the mean ± SEM (n = 6 to 12 per group; each n represents oral tissues pooled from 2 individual mice). Data are representative of 2 independent experiments. $*P < 0.05$. $**P < 0.01$. $***P < 0.001$. FACS, fluorescence-activated cell sorting; SSC, side-scattered light.
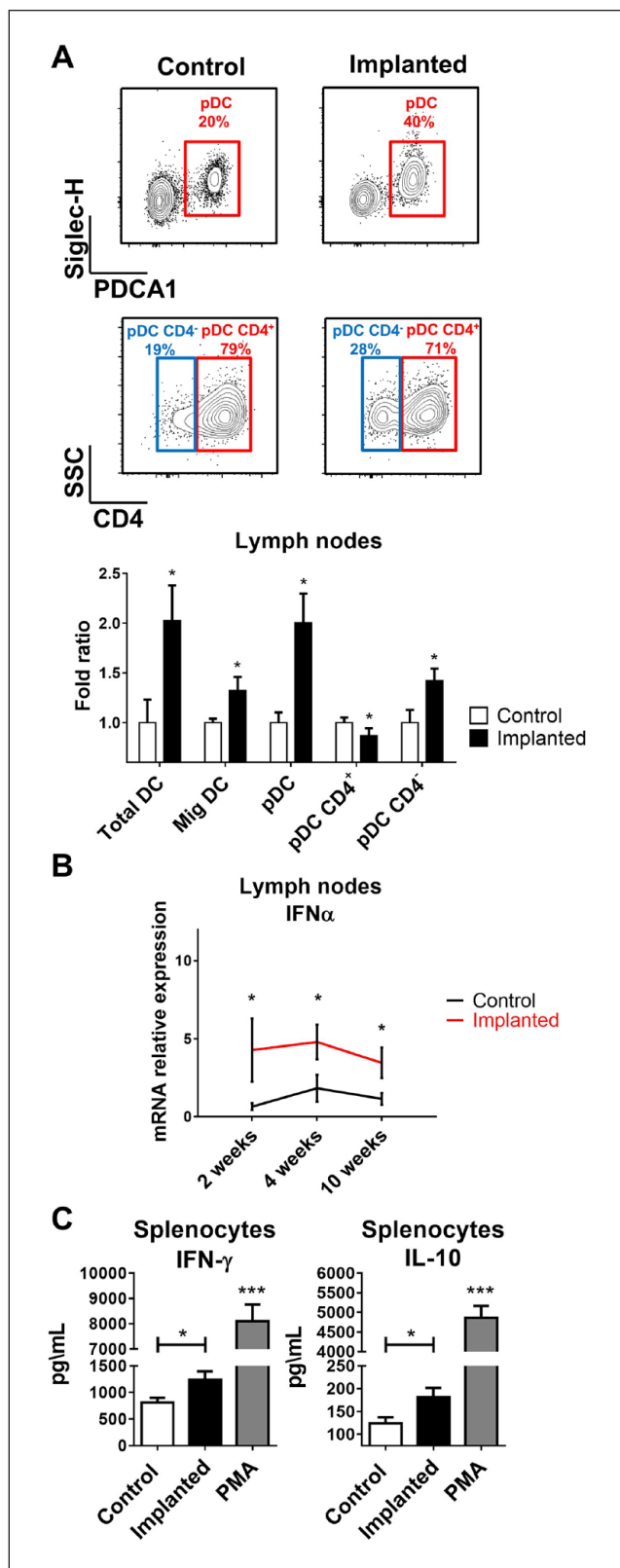
Figure 3. Increased proportions of plasmacytoid dendritic cells (pDCs) and cytokine production in the lymph nodes and spleen of implanted compared with nonimplanted mice (Control). (**A**) Representative FACS plots of lymph nodes illustrate the change in proportions of pDCs (MHCII^low CD11c^int CD11b^– B220^+ PDCA1^+ Siglec-H^+) and their CD4^– pDC subset from the parent gate. Bar graph presents the fold change in the percentage of each immune subtype from the total cell count,

inflammatory cells, such as TNF-α, VCAM-1, ICAM-1, and P/E-selectins (Appendix Fig. 1B). Taken together, implant placement results in a sustained high-leukocyte infiltration not only locally but at distant gingival sites, representing a modified homoeostatic state rather than acute inflammation. Furthermore, the differences in leukocyte subpopulations among implants and contralateral teeth suggest the development of distinct immune responses at each site that might regulate bone loss differently.

Ongoing Elevated Levels of Plasmacytoid Dendritic Cells and Cytokine Production in Implanted Mice

The presence of dysregulated gingival immunity several weeks after implant placement may imply that the implants induce prolonged activation of the immune system. To address this point, we collected the gingiva-draining lymph nodes (LNs) of naïve and implanted mice for analysis of dendritic cells (DCs). Appendix Figure 2 depicts our gating strategy employed to identify different DCs in the LNs. Increased frequencies of total DCs (CD11c^+ MHCII^+) were found in the LNs of implanted mice as compared with naïve control (Fig. 3A). This elevation was mainly attributed to accumulation of plasmacytoid dendritic cells (pDCs; MHCII^lo CD11c^int CD11b^– B220^+ PDCA1^+ Siglec-H^+) rather than migratory DCs (CD11c^int MHCII^hi) arriving from the gingiva. However, further analysis of pDCs revealed that in implanted mice, a larger fraction of these cells was CD4 negative, a phenotype previously reported to represent migratory pDCs with a capacity to secrete IFN-α (Yang et al. 2005). Indeed, using quantitative RT-qPCR, we were able to detect upregulated and sustained expression of IFN-α in the LNs of implanted mice as compared with the LNs of naïve mice (Fig. 3B). On this regard, we recently reported that elevated IFN-α production in the draining LNs induces chronic activation of T cells that facilitate bone loss (Mizraji et al. 2017). To examine whether such chronic activation is taking place also upon implant placement, we cultured splenocytes from 4-wk implanted mice with no external stimulation and measured spontaneous cytokine secretion using ELISA. Indeed, higher levels of IFN-γ and IL-10 were found in the supernatants of implanted mice as compared with naïve control, indicating that splenocytes of implanted mice are chronically activated (Fig. 3C). These findings suggest that production of IFN-α by pDCs play a role in dysregulating immunity in implanted mice via

ongoing activation of the gingiva and development of bone-destructive immune responses.

Implant Placement Results in Oral Microbial Dysbiosis

Considerable alteration of oral mucosal immunity is known to cause oral microbial dysbiosis that is often associated with pathologic consequences (Hajishengallis et al. 2011; Nassar et al. 2017). We thus examined if dysregulation of gingival immune responses by implants is also capable of altering the oral microbiota. For this, we sampled oral microbiota from the same mice before implant placement and 4 wk after. As demonstrated in Figure 4A, the levels of cultivated anaerobic and aerobic bacteria were significantly higher in implanted mice as compared with the level that they had prior to implant placement. Further analysis revealed that following implant placement, the mice had a significant increase in the diversity of oral microbiota (Fig. 4B), which also varied significantly from the microbiota that they harbored prior to implant placement (Fig. 4C). Detailed taxonomic analysis showed that while preimplanted mice were primarily colonized by the bacterial phylum Firmicutes, implant placement facilitates the expansion of Proteobacteria and Bacteroidetes on the expense of Firmicutes (Fig. 4D). On a family level, implant placement decreases the relative abundance of Streptococcaceae by 2-fold, whereas other bacteria families were expanded, such as S24-7 (Bacteroidetes), Pasteurellaceae (Proteobacteria), Clostridiales-2 (Firmicutes), Enterobacteriaceae (Proteobacteria), Bacteroidaceae (Bacteroidetes) Lactobacillaceae (Firmicutes), and more (Fig. 4E). Of note, the relative proportions of known periodontal pathogenic families, such as Prevotellaceae (Bacteroidetes), Fusobacteriaceae (Fusobacteria), and Porphyromonadaceae (Bacteroidetes), were increased after implant insertion (Fig. 4E). To understand more accurately the impact of immune dysregulation in the tissue around implants and contralateral teeth on local oral microbiota, we sampled the microbiota specifically in these sites using small microbrushes under full anesthesia and tongue retraction. Absolute abundance of key bacterial families was then analyzed by RT-qPCR of the 16S gene. Following a second taxonomic analysis, we were able to demonstrate similar changes in the microbiome of the contralateral teeth and implant groups after implant insertion (Appendix Fig. 3A). Concurring with these results, Prevotellaceae and Lactobacillaceae were increased while Streptococcaceae decreased around implants and the contralateral teeth in comparison with samples taken in an identical manner from preimplanted mice (Fig. 4F, Appendix Fig. 3B). It should be also mentioned that in correlation to the intensity of the immune dysregulation, the absolute abundance of Prevotellaceae and Streptococcaceae around implants was significantly different than that observed in the contralateral teeth. Interestingly, the changes in microbial diversity observed in implanted mice resembled microbial dysregulation observed in the oral cavity of mice lacking GAS6, a key regulator of oral mucosal homeostasis (Nassar et al. 2017). In line with this notion, we found significant reduction of GAS6 expression in the gingiva surrounding the implants and, to a lesser extent, at the contralateral gingiva as compared with the gingiva of the same mice prior to implant placement (Fig. 4G). Since GAS6-madiated effect is influenced by the ability of the expended bacteria to utilize reactive oxygen species generated under inflammatory conditions for anaerobic respiration, we also measured the expression of reactive oxygen species–producing genes *iNOS* and *DUOX2*. Indeed, the expression of both genes was upregulated in the gingiva of implanted mice and contralateral gingiva (Fig. 4H). Finally, we asked whether the oral dysbiosis induced by implants has any impact on gut microbiota. As depicted in Appendix Figure 3C, 10 wk after implant placement, considerable alteration in the diversity of the gut microbiota was detected. In conclusion, implant placement leads to expansion of bacteria that are known to expand under inflammatory conditions, while the magnitude of dysbiosis correlates to the level of inflammation induced by the implant locally or remotely. This process is likely to be mediated by the capability of the implants to activate the oral mucosa via downregulation of GAS6 expression. Additionally, the capacity of oral implants to alter the gut microbiota over time demonstrates their vast systemic influence on the host microbial and immune system.

Bone Loss around Implants but Not Contralateral Teeth Is Microbiota Independent

To dissect the role of microbiota during periodontal bone loss in implanted mice, we administered the mice with broad-spectrum antibiotics and antifungal treatment before and after implant placement, as illustrated in Figure 5A. Examination of oral microbiota during the treatment confirmed a massive reduction in the bacterial load, and the remaining bacterial population displayed significant variation from the original microbiota (Appendix Fig. 4A–F). We next quantified residual bone level around implants and revealed that the reduction in the microbiota had no impact on bone destruction, since treated mice lost implant-supporting bone similar to untreated mice (Fig. 5B). On a contrary, alveolar bone loss in the contralateral teeth was significantly inhibited by the treatment, highlighting the central role of the microbiota in this process (Fig. 5C). As these results imply that local immunity plays a critical role in bone loss around implants, we assessed implant immune responses during the treatment. Total leukocytes as well as B and CD4^{+} T lymphocytes, expressing RANKL or not, were considerably reduced due to the treatment (Fig. 5D). Nevertheless, the percentage of neutrophils was not altered by the treatment. Evaluation of DCs in gingiva-draining LNs showed a reduction of migratory DCs upon antibiotic treatment, whereas CD4^{−} pDCs retained their high percentages in implanted mice (Fig. 5E). Spontaneous secretion of IFN-γ levels by splenocytes was not affected by the antibiotic treatment, indicating that chronic activation of T cells in implanted mice is microbiota independent (Fig. 5F). In summary, although implants and contralateral teeth have dysregulated immunity and microbiota, the mechanisms mediating bone loss at each site are distinct. Whereas bone loss in contralateral teeth is
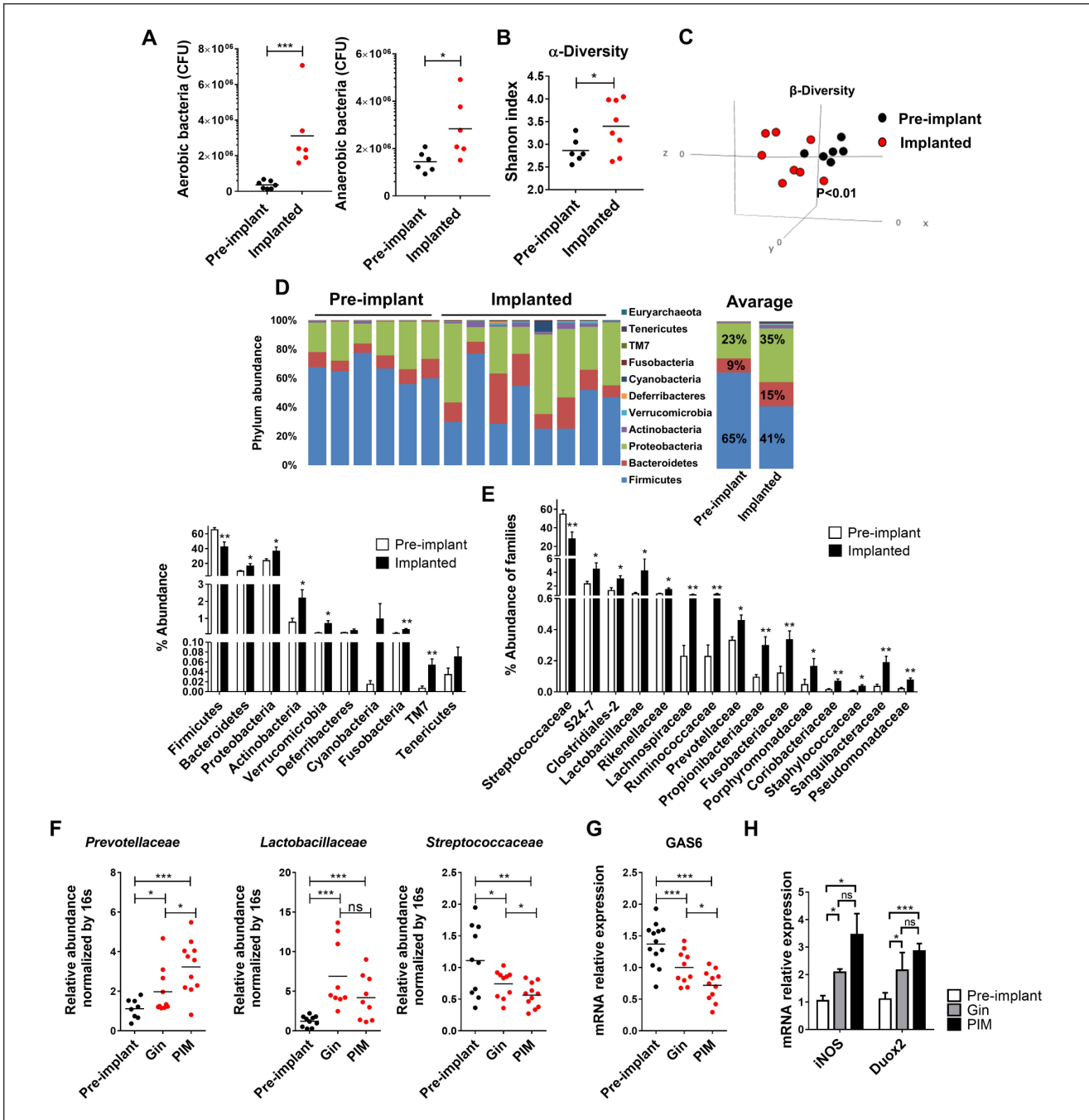
Figure 4. Bacterial dysbiosis in the oral cavity following implant placement. (**A**) Colony-forming unit (CFU) of total cultivable oral aerobic and anaerobic bacteria. Swab samples were taken before implant placement and 4 wk after implant placement. The results are shown for each mouse, with black lines denoting mean values (*n* = 6 mice per group). Representative data of 1 of 3 independent experiments are shown. (**B**) Alpha diversity dot plot representing taxa richness before and 4 wk after implant placement per the Shannon index (*n* = 6 to 8 mice per group). (**C**) Three-dimensional nonmetric multidimensional scaling plots based on Bray-Curtis dissimilarity illustrate the bacterial community structure before and 4 wk after implant insertion. Permutational multivariate analysis of variance was used to assess significance between groups. Significant clustering is observed after implant placement. Each dot represents the oral microbiome of 1 mouse. (**D**) The 10 most abundant phyla sequenced from oral swabs sampled before and after implant placement. Average chart represents the overall distribution of the abundant phyla accompanied with bar plot illustrating the relative proportion for each of the noted taxa, presented as the mean ± SEM (*n* = 6 to 8 mice per group). (**E**) Changes in bacterial families 4 wk following implant placement. Bar plot illustrating the relative proportion of significantly altered families, presented as the mean ± SEM (*n* = 6 to 8 mice per group). (**F**) Site-specific bacterial sampling was taken before and 4 wk after implant insertion from the gingiva (Gin) and the peri-implant mucosa (PIM). Dot graphs demonstrate the fold change in the gene encoding for the 16S rRNA of major bacterial families upon implant placement, normalized to 18S (*n* = 8 to 11 mice per group). Horizontal lines indicate the mean values for each group. Data are representative of 2 independent experiments. (**G**, **H**) mRNA levels of the noted genes in the gingiva were quantified per quantitative real-time polymerase chain reaction. Graphs present the fold change in gene expression normalized to the Gin group and represent the mean ± SEM (*n* = 5 to 13 per group; each *n* represents oral tissues pooled from 2 individual mice). Data are representative of 1 of 2 independent experiments. *P < 0.05. **P < 0.01. ***P < 0.001.
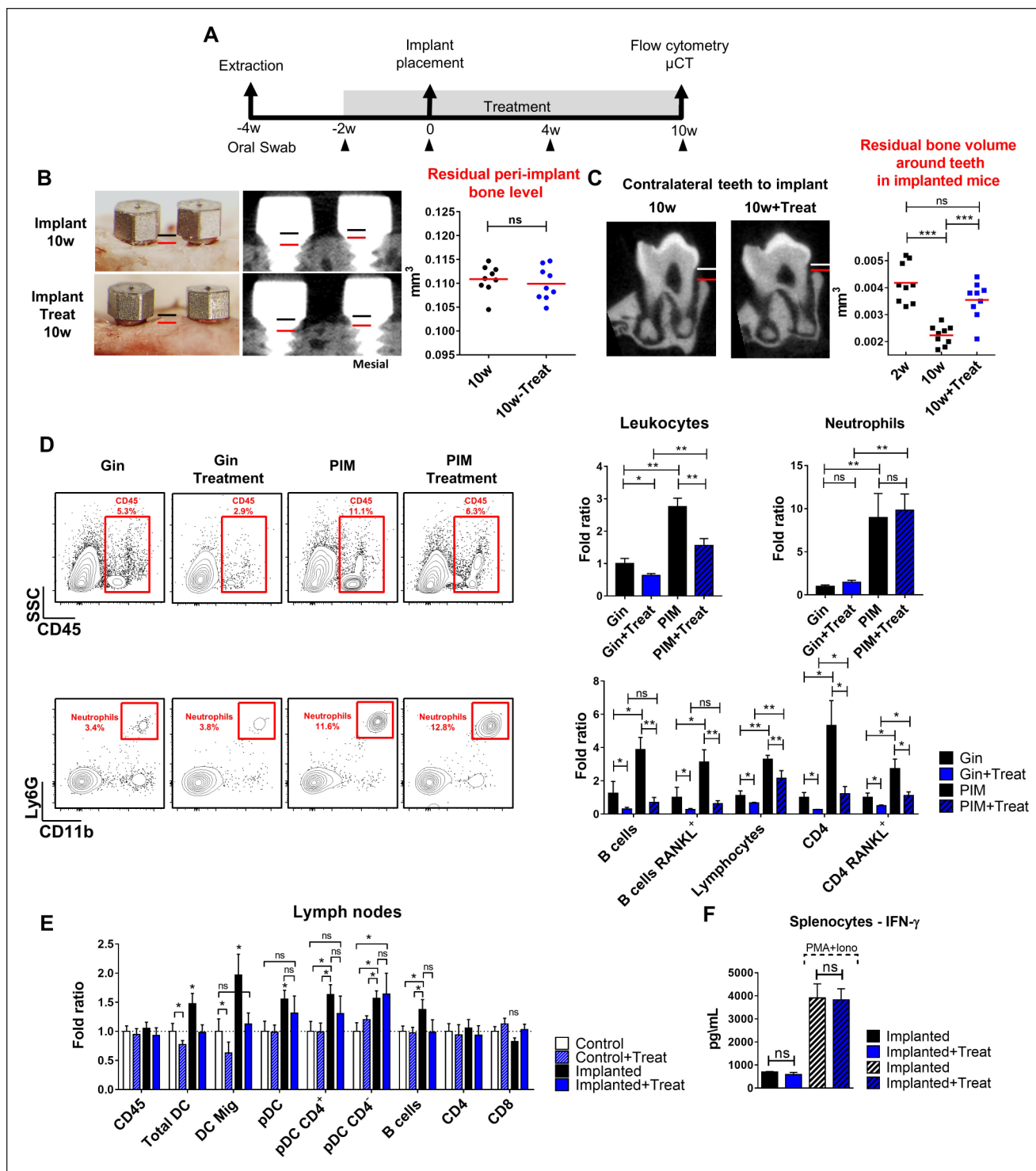
Figure 5. Bone loss around implants but not contralateral teeth is microbiota independent. (**A**) Experimental design. (**B**, **C**) Representative clinical micro–computed tomography images and 3-dimensional quantification analysis of the residual peri-implant bone and the residual bone in the contralateral teeth. Bone loss is presented as the distances between the black/white line and the red line. Residual bone volume was calculated with micro–computed tomography with 9 mice per group. Data are representative of 1 of 2 independent experiments. (**D**) Representative FACS plots illustrates the frequencies of total leukocytes (CD45+) and neutrophils (Ly6G+CD11b+) 10 wk after implant insertion, with or without treatment in the contralateral gingiva (Gin) and peri-implant mucosa (PIM) groups. Frequencies of different immune subsets were determined from the whole peri-implant and gingiva tissues. Bar graphs indicate the fold change in the percentage of each immune subset from the total cell count, normalized to the Gin group and presented as the mean ± SEM ($n = 4$ per group; each n represents tissues pooled from 2 individual mice). Data are representative of 1 of 2 independent experiments. (**E**) Lymph nodes from control and implanted mice, with or without treatment, were harvested and analyzed with flow cytometry 10 wk after implant insertion. Bar graph demonstrates the fold change in frequencies of different immune cells from total cell counts, normalized to the control group and presented as the mean ± SEM ($n = 6$ mice per group). Data are representative of 1 of 2 independent experiments. (**F**) IFN-γ levels in the supernatants of cultured splenocytes extracted from implanted mice with or without treatment. For positive control, the cells were cultured in the presence of PMA and ionomycin. Bar graphs presented as the mean ± SEM ($n = 7$ mice per group). *$P < 0.05$. **$P < 0.01$. ***$P < 0.001$. FACS, fluorescence-activated cell sorting; SSC, side-scattered light.

microbiota dependent, around implants this process is microbiota independent and likely to involve chronic immune activation mediated by IFN-α secreting pDCs.

Discussion

This study expands our previous observations demonstrating that, besides dysregulating local immunity (Heyman et al. 2018), dental implants have a broader influence on oral mucosal immunity. The data demonstrate that implant-associated immune responses dysregulate oral microbiota, which in turn alters gingival immunity at distant sites and facilitates alveolar bone loss. Such remote bone loss, however, involves distinct mechanisms than bone loss around implants, as it is induced by the microbiota and can be prevented by antibiotic treatment. Destruction of alveolar bone due to a dysbiotic microbiome was reported in experimental and human periodontitis and was mediated by expansion of IL-17–producing T cells (Th17) and recruitment of neutrophils (Dutzan et al. 2018). A study further reported that such Th17 cells are in fact FoxP3$^+$ T cells that were converted locally to Th17 and thus termed *exFoxP3Th17 cells* (Tsukasaki and Takayanagi 2019). This, however, does not seem to be the mechanism of remote bone loss in the present study, since 1) IL-17 expression and neutrophils were not elevated in contralateral gingiva and 2) Foxp3$^+$ T cells were elevated. This is also the case of implant-specific bone loss, because IL-17 and neutrophils that were considerably increased around implants led to a dysbiotic microbiota and not vice versa. Therefore, bone loss induced by dental implants, either locally or remotely, is mediated by an alternative mechanism that differs from periodontitis-associated bone destruction.

A possible mechanism to implant-associated bone loss could be the prolonged secretion of type I interferons (e.g., IFN-α and IFN-β), which was previously shown to induce chronic inflammation and tissue destruction (Wilson et al. 2013). Furthermore, using a model of repetitive infections with *Porphyromonas gingivalis*, we previously reported protracted and high levels of pDCs and type I interferons, which resulted in elevated T-cell activation, high RANKL expression, and alveolar bone loss (Mizraji et al. 2017). This pathologic process was reversed by depletion of type I interferons, demonstrating the deleterious impact of unrestrained expression of these cytokines on oral immunity. Accordingly, the durable high levels of pDCs and IFN-α/β in the LNs and the upregulation of gingival IFN-α/β in implanted mice might explain the chronic activation of T and B cells and their elevated RANKL expression that facilitate bone loss around implants. Elevation of RANKL-expressing T cells was also detected in the contralateral gingiva as well as upregulation of IFN-γ mRNA levels. This raises the possibility that excessive Th1 responses rather than Th17 cells mediate bone loss in remote sites as previously suggested (Teng et al. 2005; Arizon et al. 2012; Mizraji et al. 2018). Nonetheless, gingival IFN-α/β levels were shown to be negatively regulated by GAS6 expressed in epithelial cells (Nassar et al. 2017), and in agreement with this notion, reduced expression of GAS6 was detected in the gingiva of implanted mice. It is worth mentioning that activation of pDCs could be mediated by the reported capacity of particles and titanium ions released by the implant to dysregulate the oral microbiota (Souza et al. 2020). This might lead to changes in the accessibility of bacterial DNA that can be sensed by TLR9 in pDCs and induce secretion of type I interferons (Colonna et al. 2004).

The nature of oral microbiota is known to reflect the immunologic status of the oral mucosa (Hajishengallis et al. 2012; Costalonga and Herzberg 2014). Indeed, we found in implanted mice an expansion of oral bacteria that are capable to utilize inflammation by-products for anaerobic respiration (Winter et al. 2013; Winter and Baumler 2014). In fact, the dysbiosis observed in implanted mice resembles that found in *Gas6$^{-/-}$* mice, further supporting a role to the GAS6–type I interferon axis in our system (Nassar et al. 2017). Detailed taxonomic analysis also revealed that microbial dysregulation is niche specific, as the predominant changes in the microbiota were found around implants as compared with remote gingiva. Nevertheless, the relatively moderate microbial changes observed in remote sites were sufficient to accelerate alveolar bone loss, highlighting the delicate equilibrium of bone remodeling in the periodontium. It is not completely clear yet which mechanisms are induced in remote sites by the microbiota that facilitate bone loss. However, based on cytokine expression in the gingiva and lymphocyte infiltration, it is likely that Th1 immune responses represented by IFN-γ are involved in this process rather than Th17 responses. Interestingly, besides altering the oral microbiota, dental implants induce microbial dysbiosis in the gut. This is in line with a previous study demonstrating that microbial dysbiosis initiated by periodontal pathogens is capable of dysregulating gut microbiota (Nakajima et al. 2015), highlighting the systemic impact of the oral microbiota in the body.

The higher accumulation of leukocytes and expression of proinflammatory cytokines around implants as compared with normal teeth are in concurrence with human studies (Nowzari et al. 2008; Nowzari et al. 2012; Yaghobee et al. 2014; Gurlek et al. 2017; Obadan et al. 2018). Of note, these studies showed aggressive immune responses, quick uncontrolled tissue destruction, and bone loss around implants as compared with teeth (Salvi et al. 2017), similar to the situation that we found in mice. While the aim of this study was to address the role of implant placement on oral mucosal homeostasis and bone loss, the distinct immunologic mechanisms induced around implants and remote teeth might shed light on the different responsiveness of human periodontitis and peri-implantitis to treatment (Renvert et al. 2008). It can be assumed that peri-implantitis, in contrast to periodontitis, is not responding well to mechanical and antibiotic treatments because bone loss taking place around implants is not entirely microbiota dependent. While our results are based on experiments performed in a murine model and should be cautiously interpreted to humans, they may have clinical implications suggesting that bone loss in human peri-implantitis is likely to be mediated by 2 factors: first, bacterial infection that can be treated with antibiotic; second, host destructive immunity against the implant that is microbiota independent and thus cannot be prevented by antibiotic or plaque control. As such, future treatment against peri-implantitis

might include immunotherapeutic approaches in addition to the regular treatment. Our study suggests that such approaches could target type I interferon signaling that is likely to be involved in implant bone loss in a microbiota-independent manner.

Author Contributions

O. Heyman, contributed to conception, data acquisition, and analysis, drafted and critically revised the manuscript; Y. Horev, N. Koren, O. Barel, I. Aizenbud, Y. Aizenbud, contributed to data acquisition, critically revised the manuscript; M. Brandwein, contributed to data analysis and interpretation, drafted and critically revised the manuscript; L. Shapira, contributed to conception and data interpretation, critically revised the manuscript; A.H. Hovav, A. Wilensky, contributed to conception, design, data analysis, and interpretation, drafted and critically revised the manuscript. All authors gave final approval and agree to be accountable for all aspects of the work.

Acknowledgments

References

Arizon M, Nudel I, Segev H, Mizraji G, Elnekave M, Furmanov K, Eli-Berchoer L, Clausen BE, Shapira L, Wilensky A, et al. 2012. Langerhans cells down-regulate inflammation-driven alveolar bone loss. Proc Natl Acad Sci U S A. 109(18):7043–7048.

Armitage GC. 1996. Periodontal diseases: diagnosis. Ann Periodontol. 1(1):37–215.

Berglundh T, Armitage G, Araujo MG, Avila-Ortiz G, Blanco J, Camargo PM, Chen S, Cochran D, Derks J, Figuero E, et al. 2018. Peri-implant diseases and conditions: consensus report of workgroup 4 of the 2017 World Workshop on the Classification of Periodontal and Peri-implant Diseases and Conditions. J Periodontol. 89 Suppl 1:S313–S318.

Berglundh T, Zitzmann NU, Donati M. 2011. Are peri-implantitis lesions different from periodontitis lesions? J Clin Periodontol. 38 Suppl 11:188–202.

Chen B, Wu W, Sun W, Zhang Q, Yan F, Xiao Y. 2014. RANKL expression in periodontal disease: where does RANKL come from? Biomed Res Int. 2014:731039.

Colonna M, Trinchieri G, Liu YJ. 2004. Plasmacytoid dendritic cells in immunity. Nat Immunol. 5(12):1219–1226.

Costalonga M, Herzberg MC. 2014. The oral microbiome and the immunobiology of periodontal disease and caries. Immunol Lett. 162(2 Pt A):22–38.

Derks J, Tomasi C. 2015. Peri-implant health and disease: a systematic review of current epidemiology. J Clin Periodontol. 42 Suppl 16:S158–S171.

Dutzan N, Abusleme L, Bridgeman H, Greenwell-Wild T, Zangerle-Murray T, Fife ME, Bouladoux N, Linley H, Brenchley L, Wemyss K, et al. 2017. On-going mechanical damage from mastication drives homeostatic Th17 cell responses at the oral barrier. Immunity. 46(1):133–147.

Dutzan N, Kajikawa T, Abusleme L, Greenwell-Wild T, Zuazo CE, Ikeuchi T, Brenchley L, Abe T, Hurabielle C, Martin D, et al. 2018. A dysbiotic microbiome triggers TH17 cells to mediate oral mucosal immunopathology in mice and humans. Sci Transl Med. 10(463):eaat0797.

Grimaud E, Soubigou L, Couillaud S, Coipeau P, Moreau A, Passuti N, Gouin F, Redini F, Heymann D. 2003. Receptor activator of nuclear factor kappaB ligand (RANKL)/osteoprotegerin (OPG) ratio is increased in severe osteolysis. Am J Pathol. 163(5):2021–2031.

Gurlek O, Gumus P, Nile CJ, Lappin DF, Buduneli N. 2017. Biomarkers and bacteria around implants and natural teeth in the same individuals. J Periodontol. 88(8):752–761.

Hajishengallis G, Darveau RP, Curtis MA. 2012. The keystone-pathogen hypothesis. Nat Rev Microbiol. 10(10):717–725.

Hajishengallis G, Liang S, Payne MA, Hashim A, Jotwani R, Eskan MA, McIntosh ML, Alsam A, Kirkwood KL, Lambris JD, et al. 2011.

Low-abundance biofilm species orchestrates inflammatory periodontal disease through the commensal microbiota and complement. Cell Host Microbe. 10(5):497–506.

Hajishengallis G, Moutsopoulos NM, Hajishengallis E, Chavakis T. 2016. Immune and regulatory functions of neutrophils in inflammatory bone loss. Semin Immunol. 28(2):146–158.

Heyman O, Koren N, Mizraji G, Capucha T, Wald S, Nassar M, Tabib Y, Shapira L, Hovav AH, Wilensky A. 2018. Impaired differentiation of langerhans cells in the murine oral epithelium adjacent to titanium dental implants. Front Immunol. 9:1712.

Hovav AH. 2014. Dendritic cells of the oral mucosa. Mucosal Immunol. 7(1):27–37.

Javed F, Alghamdi AS, Ahmed A, Mikami T, Ahmed HB, Tenenbaum HC. 2013. Clinical efficacy of antibiotics in the treatment of peri-implantitis. Int Dent J. 63(4):169–176.

Mizraji G, Heyman O, Van Dyke TE, Wilensky A. 2018. Resolvin D2 restrains Th1 immunity and prevents alveolar bone loss in murine periodontitis. Front Immunol. 9:785.

Mizraji G, Nassar M, Segev H, Sharawi H, Eli-Berchoer L, Capucha T, Nir T, Tabib Y, Maimon A, Dishon S, et al. 2017. *Porphyromonas gingivalis* promotes unrestrained type I interferon production by dysregulating TAM signaling via MYD88 degradation. Cell Rep. 18(2):419–431.

Nakajima M, Arimatsu K, Kato T, Matsuda Y, Minagawa T, Takahashi N, Ohno H, Yamazaki K. 2015. Oral administration of *P. gingivalis* induces dysbiosis of gut microbiota and impaired barrier function leading to dissemination of enterobacteria to the liver. PloS One. 10(7):e0134234.

Nassar M, Tabib Y, Capucha T, Mizraji G, Nir T, Pevsner-Fischer M, Zilberman-Schapira G, Heyman O, Nussbaum G, Bercovier H, et al. 2017. GAS6 is a key homeostatic immunological regulator of host-commensal interactions in the oral mucosa. Proc Natl Acad Sci U S A. 114(3):E337–E346.

Nowzari H, Botero JE, DeGiacomo M, Villacres MC, Rich SK. 2008. Microbiology and cytokine levels around healthy dental implants and teeth. Clin Implant Dent Relat Res. 10(3):166–173.

Nowzari H, Phamduong S, Botero JE, Villacres MC, Rich SK. 2012. The profile of inflammatory cytokines in gingival crevicular fluid around healthy osseointegrated implants. Clin Implant Dent Relat Res. 14(4):546–552.

Obadan F, Craitoiu S, Manolea HO, Hincu MC, Iacov-Craitoiu MM. 2018. The evaluation of the morphological evolution of the tissue integration of dental implants through conventional histology and immunohistochemistry techniques. Rom J Morphol Embryol. 59(3):851–859.

Renvert S, Roos-Jansaker AM, Claffey N. 2008. Non-surgical treatment of peri-implant mucositis and peri-implantitis: a literature review. J Clin Periodontol. 35(8 Suppl):305–315.

Romanos GE, Javed F, Delgado-Ruiz RA, Calvo-Guirado JL. 2015. Peri-implant diseases: a review of treatment interventions. Dent Clin North Am. 59(1):157–178.

Salvi GE, Cosgarea R, Sculean A. 2017. Prevalence and mechanisms of peri-implant diseases. J Dent Res. 96(1):31–37.

Souza JGS, Costa Oliveira BE, Bertolini M, Lima CV, Retamal-Valdes B, de Faveri M, Feres M, Barao VAR. 2020. Titanium particles and ions favor dysbiosis in oral biofilms. J Periodontal Res. 55(2):258–266.

Teng YT, Mahamed D, Singh B. 2005. Gamma interferon positively modulates *Actinobacillus actinomycetemcomitans*–specific RANKL+ CD4+ Th-cell-mediated alveolar bone destruction in vivo. Infect Immun. 73(6):3453–3461.

Tsukasaki M, Takayanagi H. 2019. Osteoimmunology: evolving concepts in bone-immune interactions in health and disease. Nat Rev Immunol. 19(10):626–642.

Van Dyke TE, Lester MA, Shapira L. 1993. The role of the host response in periodontal disease progression: implications for future treatment strategies. J Periodontol. 64 Suppl 8S:792–806.

Wilson EB, Yamada DH, Elsaesser H, Herskovitz J, Deng J, Cheng G, Aronow BJ, Karp CL, Brooks DG. 2013. Blockade of chronic type I interferon signaling to control persistent LCMV infection. Science. 340(6129):202–207.

Winter SE, Baumler AJ. 2014. Why related bacterial species bloom simultaneously in the gut: principles underlying the "like will to like" concept. Cell Microbiol. 16(2):179–184.

Winter SE, Lopez CA, Baumler AJ. 2013. The dynamics of gut-associated microbial communities during inflammation. EMBO Rep. 14(4):319–327.

Yaghobee S, Khorsand A, Rasouli Ghohroudi AA, Sanjari K, Kadkhodazadeh M. 2014. Assessment of interleukin-1beta and interleukin-6 in the crevicular fluid around healthy implants, implants with peri-implantitis, and healthy teeth: a cross-sectional study. J Korean Assoc Oral Maxillofac Surg. 40(5):220–224.

Yang GX, Lian ZX, Kikuchi K, Liu YJ, Ansari AA, Ikehara S, Gershwin ME. 2005. CD4-plasmacytoid dendritic cells (pDCs) migrate in lymph nodes by CpG inoculation and represent a potent functional subset of pDCs. J Immunol. 174(6):3197–3203.